

## Pressure Effects on the Lateral Distribution of Cholesterol in Lipid Bilayers: A Time-Resolved Spectroscopy Study

Patrick Tauc,\* C. Reyes Mateo,# and Jean-Claude Brochon\*

\*Laboratoire de Biochimie Moléculaire et Cellulaire, CNRS, Université Paris-Sud, 91405 Orsay, France, and #Instituto de Química-Física "Rocasolano," C.S.I.C. 28020 Madrid, Spain

**ABSTRACT** The effects of hydrostatic pressure and temperature on the phase behavior and physical properties of the binary mixture palmitoylcholine/cholesterol, over the 0–40 molar % range of cholesterol compositions, were determined from the changes in the fluorescence lifetime distribution and anisotropy decay parameters of the natural lipid *trans*-parinaric acid (*t*-PnA). Pressurized samples were excited with a Ti-sapphire subpicosecond laser, and fluorescence decays were analyzed by the quantified maximum entropy method. Above the transition temperature ( $T_T = -5^\circ\text{C}$ ), at atmospheric pressure, two liquid-crystalline phases,  $\alpha$  and  $\beta$ , are formed in this system. At each temperature and cholesterol concentration below the transition pressure, the fluorescence lifetime distribution pattern of *t*-PnA was clearly modulated by the pressure changes. Pressure increased the fraction of the liquid-ordered  $\beta$ -phase and its order parameter, but it decreased the amount of cholesterol in this phase. Palmitoylcholine/cholesterol phase diagrams were also determined as a function of temperature and hydrostatic pressure.

### INTRODUCTION

The "fluid mosaic" model of Singer and Nicolson (1972) for biological membranes describes the organization and structure of the bilayer as an agglomerate of lipid and proteins in a fluid-like random structure. However, certain studies carried out in the last decade on natural membranes (Gordon et al., 1983; Wolf and Voglmayr, 1984; Yechiel and Edidin, 1987; for a review see Alvia et al., 1988) have suggested that a nonuniform distribution of lipids may give rise to specialized domains in the cell surface membrane. These membrane domains most likely derive from the presence of many different species of lipids and proteins that are immiscible. Cholesterol has a particular chemical structure that is very different from the other lipid components of natural membranes. It has become increasingly evident that this molecule is not randomly distributed in either model membranes (Recktenwald and McConnell, 1981; Sankaram and Thompson, 1990; Vist and Davis, 1990; Almeida et al., 1992; Mateo et al., 1995) or biological membranes (Gordon et al., 1983; Mateo et al., 1991; Schroeder et al., 1991). Instead, cholesterol appears to be organized in cholesterol-rich and -poor domains. The structure and properties of these domains could affect the function of selected membrane proteins differentially distributed in one or the other type of domain.

The size and physical properties of lipid domains can be modulated by modifications in the chemical composition of

the membrane or by changes in thermodynamic parameters such as temperature and hydrostatic pressure. In a recent work (Mateo et al., 1995) we have detected, from the changes observed in the lifetime distributions of the fluorescent fatty acid *trans*-parinaric acid (*t*-PnA), the presence of two liquid-crystalline phases,  $\alpha$  and  $\beta$ , in saturated and unsaturated phospholipid/cholesterol mixtures. The study shows how temperature and cholesterol concentration modulate the formation, composition, and physical properties of these phases. In the present work we use the same experimental methodology to investigate the influence of hydrostatic pressure (below the transition pressure) on these lipid mixtures. The results show that pressure induces and increases the fraction of the liquid-ordered  $\beta$ -phase and its order parameter, but it decreases the amount of cholesterol in this phase. This work compares the different effects induced by temperature, hydrostatic pressure, and cholesterol concentration on the lipid bilayers.

### MATERIALS AND METHODS

#### Sample preparation

*t*-PnA was obtained from Molecular Probes (Eugene, OR) and used without additional purification. Purity was checked by both absorption and emission spectroscopy. Palmitoylcholine (POPC) was obtained from Sigma Chemical Co. (St. Louis, MO) and used as supplied. Stock solutions of *t*-PnA were prepared in ethanol and stored in the dark at  $-20^\circ\text{C}$  before use. The stock solution was vigorously bubbled with nitrogen before the tube was capped.

Multilamellar lipid vesicles were prepared by resuspending the appropriate amounts of dried lipid in phosphate buffer (pH 7), then heating the suspension above the phase transition temperature and vortexing. Large unilamellar vesicles (LUVs), with a mean diameter of 90 nm, were prepared from the multilamellar vesicles by extrusion techniques through Nucleopore filters with 100-nm pore size (Hope et al., 1985). The dried cholesterol-phospholipid mixtures were prepared by dissolving the weighed components in a small volume of chloroform and evaporating the solvent under a stream of nitrogen. Aliquots of *t*-PnA were added from the

Received for publication 16 December 1996 and in final form 12 December 1997.

Address reprint requests to Dr. Jean-Claude Brochon, Laboratoire de Biochimie Moléculaire et Cellulaire, CNRS, Photobiologie Moléculaire, ENS de Cachan, 61, Av. Pt Wilson, 94235 Cachan Cedex, France. Tel.: 33-1-4740-2717; Fax: 33-1-4740-2479; E-mail: brochon@lbpa.ens-cachan.fr.

© 1998 by the Biophysical Society

0006-3495/98/04/1864/07 \$2.00

stock solution directly into the unilamellar vesicle dispersions bubbled with a stream of nitrogen. The samples were stirred at 40°C to enhance the incorporation of the probe into the lipid bilayer. The final molar ratio of probe to lipid was 1:200.

## Fluorescence measurements

Time-resolved fluorescence and fluorescence anisotropy decays under pressure were recorded with a high-pressure optical cell mounted in a time-correlated single photon counting fluorometer, as described by Mateo et al. (1993b). For a strict comparison, the fluorescence decays at atmospheric pressure were also measured with this pressure optical cell. The excitation light pulse source was a Ti:sapphire subpicosecond laser (Spectra Physics) associated with a third harmonic generator tuned at 300 nm. Fluorescence emission, detected through a monochromator (Jobin-Yvon H 10) set at 405 nm ( $\Delta\lambda = 8$  nm), was achieved by means of a microchannel plate photomultiplier (Hamamatsu R1564U-06). The instrumental response function of the laser pulse (100 ps) was recorded from the same sample by detecting at  $\sim 300$  nm the light scattered from the liposomes. The stability of the laser intensity was routinely better than 5%, and the excitation peak position was better than 10 ps.

The time scaling was 20 and 40 ps per channel, and 2048 channels were in use. The anisotropy decay  $r(t)$  was extracted from the parallel  $I_{\parallel}(t)$  and perpendicular  $I_{\perp}(t)$  polarized fluorescence decay components elicited by vertically polarized excitation. The polarized components were collected alternately by rotating the analyzer polarizer every 40 s over 30 periods. Corrections were made for strain birefringence of the quartz windows of the pressure optical cell at every pressure and temperature and for monochromator transmission. The corresponding experimental G-factor =  $I_{\parallel}/I_{\perp}$  was determined from *t*-PnA in ethanol under the same conditions. Total fluorescence intensity,  $I(t)$ , was recorded by orientating the emission polarizer at the “magic” angle of 54.75° or by summing the parallel and twice the corrected perpendicular components.

## Analysis and interpretation of data

Analysis of the total fluorescence intensity  $I(t)$  was performed using the PULSE5 program (MaxEnt Solutions, Cambridge, England), based on the quantified maximum entropy method (QMEM) (Brochon, 1994; Livesey and Brochon, 1987), as described by Mateo et al. (1995). The method does not use a  $\chi^2$  statistic or entropy itself as selectors to pick out the “best” of a family of distributions, but the most probable of a complete family of solutions. It comes with a complete probability distribution of solutions surrounding the maximum. This allows error bars to be calculated (Gull, 1989; Skilling, 1991). In practice, 100 equally spaced values on the  $\tau$  scale, between 0.2 and 50 ns, were used. Because we have no prior information about the number, positions, and relative importance of lifetimes before running the data analysis, all 100 lifetimes have the same prior probability, and the program starts with a flat distribution.

After a data noise estimate, the program iterates down the entropy trajectory in optimizing the posterior inference. A termination criterion is in action when the computed probability family of solution appears to be sufficiently close to correct, i.e., the optimal probability is reached, indicating that the algorithm should be stopped (Skilling, 1989; Gull, 1989).

The anisotropy decay of *t*-PnA in lipid systems in which different environments coexist was fit by the “associated” model detailed in Mateo et al. (1995), in which the lifetime parameters of the total intensity decay are specifically associated with individual anisotropy parameters. In this model  $r(t)$  is approximated by assuming two probe populations that are characterized by specific fluorescence decay,  $I_{\alpha}(t)$  and  $I_{\beta}(t)$ , respectively, and anisotropy decay,  $r_{\alpha}(t)$  and  $r_{\beta}(t)$ , respectively. The fluorescence decay for each probe population is described by a sum of exponentials. The respective anisotropy decay is defined by a single rotational correlation time  $\phi$  plus a residual anisotropy  $r_{\infty}$ .

The fraction of  $\beta$ -phase in the bilayer can be quantified from the expression

$$K_p^{\beta/\alpha} = \frac{\chi_p^{\beta}/\chi_p^{\alpha}}{\chi_p^{\beta}/\chi_p^{\alpha}} \quad (1)$$

where  $K_p^{\beta/\alpha}$  is the partition coefficient of the probe between the  $\beta$ - and  $\alpha$ -phases, and  $\chi_p^{\beta}$  and  $\chi_p^{\alpha}$  are the fraction of probe localized in each phase, respectively. These fractions can be estimated from the amplitudes of the total fluorescence decay (see Mateo et al., 1995) if the radiative rate constants and extinction coefficients of the probe are similar in the two phases.

The second rank order parameter  $\langle P_2 \rangle$  of a fluorescent probe with cylindrical symmetry (emission and transition moments assumed parallel) for which the equilibrium angular distribution function is preserved when the molecules are pumped to the emitting state (Naqvi, 1981) is related to the residual anisotropy  $r_{\infty}$  in such macroscopically unoriented vesicle systems by

$$r_{\infty} = r_0 \langle P_2 \rangle [P_2(\cos \theta)]^2 \quad (2)$$

where  $P_2(\cos \theta)$  is the second-order Legendre polynomial for the angle  $\theta$  between the transition moments and the unique (long) inertial axis of the probe.

In this work a value of  $r_0 = 0.390$  (Hudson and Cavalier, 1988) was used for *t*-PnA, and the angle was taken as 0° to simplify the analysis, although its value should be close to 20° (Shang et al., 1991).

## RESULTS

### Pressure effects on POPC/cholesterol mixtures detected by *t*-PnA fluorescence

#### Pure POPC

The effect of hydrostatic pressure on the fluorescence intensity decay of *t*-PnA in LUV of pure POPC was measured at 20°C, 30°C, and 40°C (Table 1). At atmospheric pressure the lifetime distribution showed, in most cases, three components, with a long lifetime component varying from 3 to 6 ns, depending on temperature. In some cases the intermediate lifetime component could not be resolved, and the

**TABLE 1** Fluorescence intensity decay parameters recovered by QMEM of *t*-PnA in large unilamellar vesicles of POPC as a function of pressure and temperature

<i>T</i> (°C)	<i>P</i> (bar)	$\alpha_1$ ±0.07	$\tau_1$ (ns) ±0.3	$\alpha_2$ ±0.07	$\tau_2$ (ns) ±0.8	$\alpha_3$ ±0.07	$\tau_3$ (ns) ±0.7
20	1	0.24	0.8	0.21	1.9	0.55	6.1
	300	0.11	0.4	0.34	1.6	0.54	6.1
	500	0.14	0.9	0.19	2.8	0.67	8.0
	600	0.21	0.3	0.29	1.7	0.50	6.6
	800			0.21	1.8	0.79	7.9
	900			0.38	1.6	0.62	7.4
30	1	0.37	1.1			0.63	3.8
	300	0.38	1.3			0.62	4.5
	600	0.38	1.5			0.62	4.8
	800	0.40	1.6			0.60	5.1
	1	0.23	0.5	0.22	1.3	0.53	3.0
40	300	0.23	0.4	0.24	1.1	0.50	3.1
	600	0.20	0.3	0.30	1.1	0.50	3.2
	800	0.15	0.5	0.25	1.1	0.59	3.4

$\alpha_i$  and  $\tau_i$  are the integrated relative amplitude and barycenter value, respectively, of each lifetime component.

**TABLE 2** Fluorescence intensity decay parameters recovered by QMEM of *t*-PnA in large unilamellar vesicles of POPC at 20°C as a function of pressure and mole fraction cholesterol

$\chi_{\text{chol}}$	$P$ (bar)	$\alpha_1$ $\pm 0.07$	$\tau_1$ (ns) $\pm 0.3$	$\alpha_2$ $\pm 0.07$	$\tau_2$ (ns) $\pm 0.8$	$\alpha_3$ $\pm 0.07$	$\tau_3$ (ns) $\pm 0.7$	$\alpha_4$ $\pm 0.04$	$\tau_4$ (ns) $\pm 2$	$\chi^\beta$ $\pm 0.08$
0.05	1	0.24	0.9	0.22	3.2	0.54	7.4			0
	300	0.29	0.7	0.35	2.1	0.30	6.3	0.04	12	0.08
	600	0.14	0.9	0.31	2.1	0.47	6.5	0.08	12	0.16
	800			0.50	1.7	0.33	6.1	0.16	15	0.31
	900	0.12	0.6	0.28	1.7	0.30	7.4	0.30	11	0.59
0.10	1	0.18	0.8	0.26	2.6	0.54	7.6	0.02	15	0.39
	300	0.25	0.7	0.38	2.4	0.32	7.7	0.05	15	0.10
	600	0.15	0.7	0.41	2.3	0.26	7.4	0.19	14	0.38
0.15	1	0.20	1.3	0.23	3.1	0.41	7.7	0.16	12	0.31
	300	0.08	0.3	0.32	1.7	0.25	5.0	0.35	11	0.69
	600	0.12	0.7	0.31	2.2	0.20	5.3	0.37	13	0.73
	800	0.19	1.3			0.28	4.0	0.53	15	1.04
0.20	1	0.19	1.0	0.14	2.6	0.34	7.2	0.33	13	0.65
	300	0.26	1.3			0.25	4.2	0.49	13	0.96
	600	0.09	0.7	0.14	1.8	0.22	4.0	0.54	14	1.06
	800			0.10	1.9	0.21	5.4	0.69	15	1.35
0.30	1	0.23	1.1	0.06	3.2	0.24	6.8	0.47	13	0.92
	300			0.26	2.0	0.24	7.0	0.50	16	0.98
	600			0.27	2.0	0.23	7.0	0.50	18	0.98
	800	0.25	1.7	0.25	3.8			0.50	18	0.98
0.40	1	0.13	1.6			0.33	6.0	0.54	14	1.06

$\alpha_i$  and  $\tau_i$  are the integrated relative amplitude and barycenter value, respectively, of each lifetime component.  $\chi^\beta$  is the fraction of  $\beta$ -phase determined from  $\alpha_4$  (see text).

lifetime distribution was bimodal (Mateo et al., 1993a,b). Increasing the pressure to 900 bars did not modify the pattern of the lifetime distribution, and only the center location of the lifetime peaks was shifted to longer values.

#### POPC/cholesterol mixtures

The effects of pressure on the fluorescence intensity decay of *t*-PnA in POPC/cholesterol mixtures was measured isothermally as a function of cholesterol concentration (0–40 mol%) at 20°C, 30°C, and 40°C. The results are shown in Tables 2 and 3 and Figs. 1–3. At low cholesterol concentration and atmospheric pressure, the fluorescence decay was described by a lifetime distribution similar to that obtained in pure POPC. This pattern was modified with increasing cholesterol concentration with the appearance, at a specific cholesterol concentration, of a new lifetime component ( $\tau_4$ ) centered at longer times (9–14 ns). The amplitude of this component ( $\alpha_4$ ) increased with increasing cholesterol concentration and reached maximum at specific cholesterol levels, depending on temperature (Table 2). Based on the experiments carried out with *t*-PnA in the dimyristoylphosphatidylcholine/cholesterol and POPC/cholesterol mixed bilayers (Mateo et al., 1995),  $\alpha_4$  was associated with the fraction of probe located in  $\beta$ -phase,  $\chi_p^\beta$ . This fraction was determined from  $\alpha_4$ , assuming that  $\chi_p^\beta = 1$  when  $\alpha_4$  reaches its maximum value. At 10°C (data not

shown)  $\alpha_4$  reached values of 0.30, 0.34, 0.53, 0.51, and 0.48 at 5, 10, 15, 20, and 30 mol% cholesterol concentration, respectively. Above 20 mol% cholesterol the lipid system is exclusively  $\beta$ -phase (Mateo et al., 1995). On the other hand, at 20°C and 40 mol% cholesterol, where the lipid bilayer is also, presumably, in  $\beta$ -phase,  $\alpha_4$  was 0.54 (Table 1). From these results we have assumed a value of  $\alpha_4 = 0.51 \pm 0.04$  as the “saturating” long lifetime amplitude. Increasing the pressure to 800 bars resulted in a double effect on the lifetime distributions. Results obtained at 20°C are shown in Table 2. At low cholesterol concentrations pressure induced the appearance of a new lifetime component ( $\tau_4$ ) similar to that generated when cholesterol concentration was increased at atmospheric pressure. At higher cholesterol concentrations, where the  $\alpha$ - and  $\beta$ -phases coexist (Mateo et al., 1995), pressure increased the relative amplitude of the long lifetime component  $\tau_4$ , reaching a maximum value at  $\alpha_4 \approx 0.5$ , close to the “saturating” long lifetime amplitude obtained at atmospheric pressure. The amplitude of the short and intermediate lifetime components did not show any obvious dependence with pressure. In some cases, the peaks of the fluorescence lifetime distribution could not be sharply resolved, giving exceptionally high  $\alpha_4$  values. Experiments carried out at 900 bars and 15% and 20 mol% cholesterol, moreover, showed a very long lifetime of  $\sim 30$  ns with very small relative amplitudes, which could indicate the rising of the gel phase (data not shown). At 30°C and 40°C the effect

**TABLE 3** Integrated relative amplitude  $\alpha_4$  and barycenter value,  $\tau_4$ , recovered by MEM, of the longest lifetime component of *t*-PnA in large unilamellar vesicles of POPC as a function of pressure and mole fraction cholesterol

$\chi_{\text{chol}}$	$P$ (bar)	$T = 30^\circ\text{C}$			$T = 40^\circ\text{C}$		
		$\alpha_4$ $\pm 0.04$	$\tau_4$ (ns) $\pm 2$	$\chi^\beta$ $\pm 0.08$	$\alpha_4$ $\pm 0.04$	$\tau_4$ (ns) $\pm 2$	$\chi^\beta$ $\pm 0.08$
0.05	1			0			0
	300			0			0
	600	0.06	11	0.12	0.03	12	0.06
	800	0.11	10	0.22	0.04	11	0.08
0.10	1			0			0
	300			0			0
	600	0.13	8	0.25	0.08	7	0.16
0.15	1	0.05	10	0.10			0
	300	0.10	10	0.20			0
	600	0.26	10	0.51	0.05	9	0.10
	800	0.34	9	0.67	0.20	7	0.39
0.20	1	0.15	10	0.29	0.05	9	0.10
	300	0.21	9	0.41			
	600	0.22	11	0.43	0.11	9	0.22
	800	0.36	10	0.71	0.25	8	0.49
0.30	1	0.40	11	0.78	0.07	9	0.14
	300	0.45	10	0.88			
	600	0.50	13	1	0.21	9	0.41
	800	0.50	18	1	0.39	8	0.76
0.40	1	0.42	11	0.82	0.28	9	0.55
	300				0.33	8	0.65

$\chi^\beta$  is the fraction of  $\beta$ -phase determined from  $\alpha_4$  (see text).

of pressure on the fluorescence lifetime distribution was similar to that observed at  $20^\circ\text{C}$  (Fig. 2 and 3). The short and intermediate lifetime components did not reveal clear dependence with pressure, and only the amplitude of the long lifetime component increased with increasing pressure, decreasing temperature, or with increasing cholesterol content (Table 3).

### Pressure effects on POPC/cholesterol mixtures detected by *t*-PnA anisotropy

Fluorescence anisotropy decay of *t*-PnA in POPC/cholesterol mixtures was recorded at  $20^\circ\text{C}$  at atmospheric pressure, 500 bars, and 900 bars. In pure POPC, the analysis of data yielded one rotational correlation time and a residual anisotropy  $r_\infty$  at the three pressures studied (Table 4). In the range of pressure and cholesterol concentration where the fluorescence lifetime distribution showed a long lifetime component (see Tables 2 and 3), the anisotropy decay was relatively well fitted by using a single population model ( $\chi^2 \approx 1.3$ – $1.6$ ); however, a double population model clearly gave a better fit. Because the fluorescence lifetime distributions suggest the coexistence of  $\alpha/\beta$ -phases, we can conclude that a double population model is closer to being correct. Using the simplest approximation, the longest lifetime component of the fluorescence distribution was associated with the fluorescence decay of the probe in the  $\beta$ -phase, whereas the intermediates and short lifetimes were

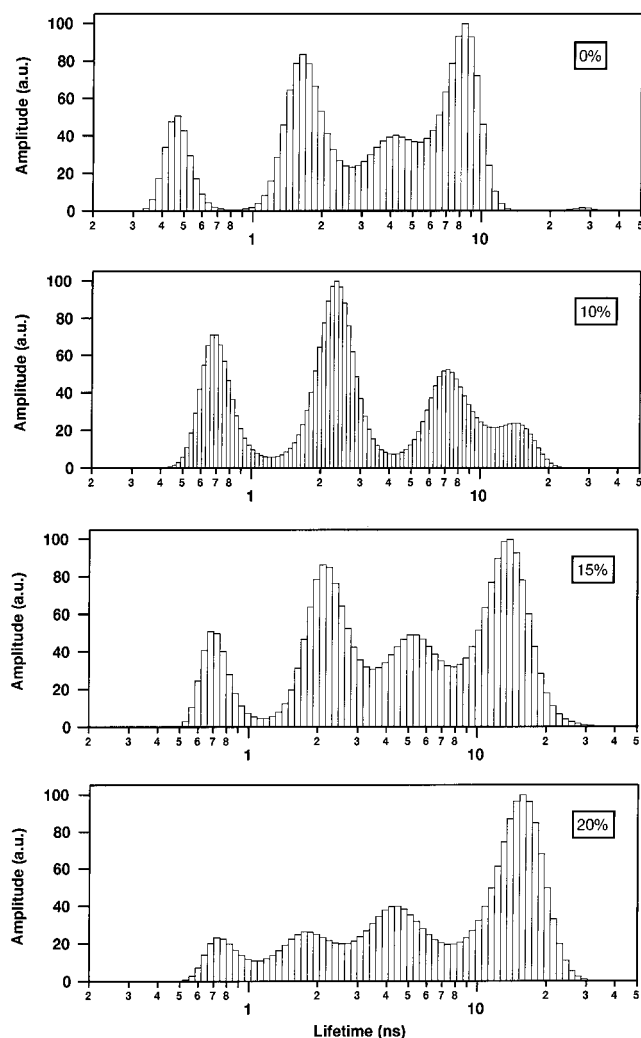


**FIGURE 1** Effect of cholesterol on the fluorescence lifetime distribution of *t*-PnA in POPC large unilamellar vesicles at  $20^\circ\text{C}$  and 600 bars.

associated with the fluorescence decay of the probe in the  $\alpha$ -phase. This is not completely correct, because at high cholesterol concentrations, where the lipid system is exclusively  $\beta$ -phase, the short and intermediate lifetime components are also detected. More complex models, obtained by associating, partially, these intermediates and short lifetimes with the emission of the probe in the  $\beta$ -phase, did not improve the fit and did not have a great influence on the anisotropy parameters obtained. The residual anisotropies  $r_\infty^\alpha$  and  $r_\infty^\beta$  and correlation times  $\phi^\alpha$  and  $\phi^\beta$  are shown in Table 4, together with the  $\chi^2$  values of the fits. The effect of pressure was essentially to induce the formation of the  $\beta$ -phase, as observed from the fluorescence decay experiments. At 900 bars and 20 mol% cholesterol, where, presumably, the membrane is in the  $\beta$ -phase, the anisotropy decay could not be well analyzed, assuming only a single probe population, and the “associative” model had to be used to properly fit the data. The large value of the highest residual anisotropy indicates that at this pressure the gel phase is rising in the membrane and coexists with the

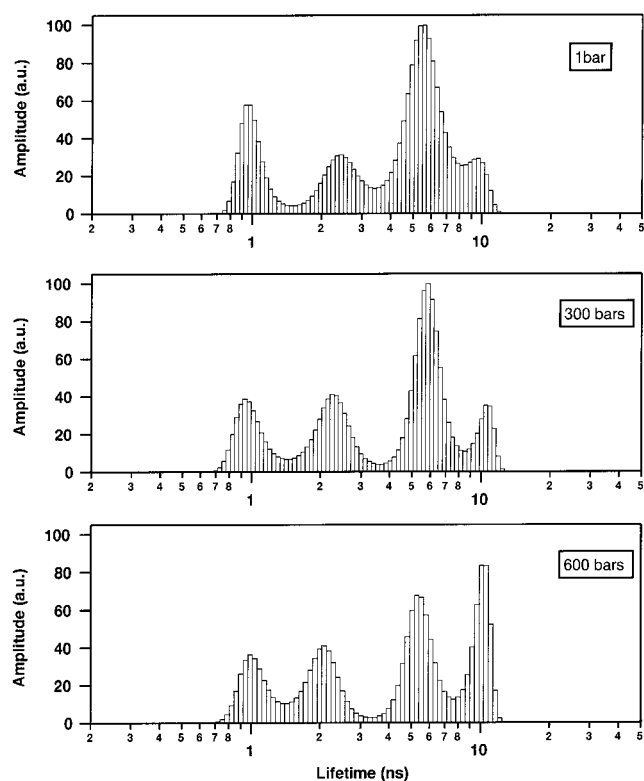


FIGURE 2 Effect of pressure on the lifetime distribution of *t*-PnA in POPC large unilamellar vesicles containing 15 mol% cholesterol at 30°C.

$\beta$ -phase. Order parameters of the probe in the lipid mixture were determined from  $r_\infty$  values by using Eq. 2 and are shown in Table 4.

## DISCUSSION

Fluorescence lifetime distribution and anisotropy results indicate that pressure, up to 800 bars, induces in the fluid phase of POPC/cholesterol mixtures the formation of the liquid-ordered  $\beta$ -phase and increases the fraction of this phase in a manner similar to that induced by decreasing temperature. At atmospheric pressure, *trans*-parinaric acid accumulates in the  $\beta$ -phase of POPC/cholesterol mixtures with a partition coefficient  $K_p^{\beta/\alpha} \approx 1$  (Mateo et al., 1995). By Eq. 1, the  $\beta$ -phase fraction,  $\chi^\beta$ , in the lipid mixture is equal to the fraction of probe located in this phase:  $\chi^\beta = \chi_p^\beta$ . In the pressurized lipid mixtures this equivalence should only be correct if  $K_p^{\beta/\alpha}$  remains invariant as a function of pressure. An increase in  $K_p^{\beta/\alpha}$  could explain the growth of  $\alpha_4$  as pressure is increased; however, it cannot justify the apparition of this component. With our instrumentation it was not possible to verify that the same  $K_p^{\beta/\alpha}$  is preserved at high pressures; however, it seems reasonable, because no systematic temperature dependence was observed for *t*-PnA partition coefficients (Welti and Silbert, 1982). Following this hypothesis,  $\chi^\beta$  was calculated at each temperature, pressure, and cholesterol concentration (see Tables 1–3) from  $\alpha_4$ , assuming, as was described in the Results, that

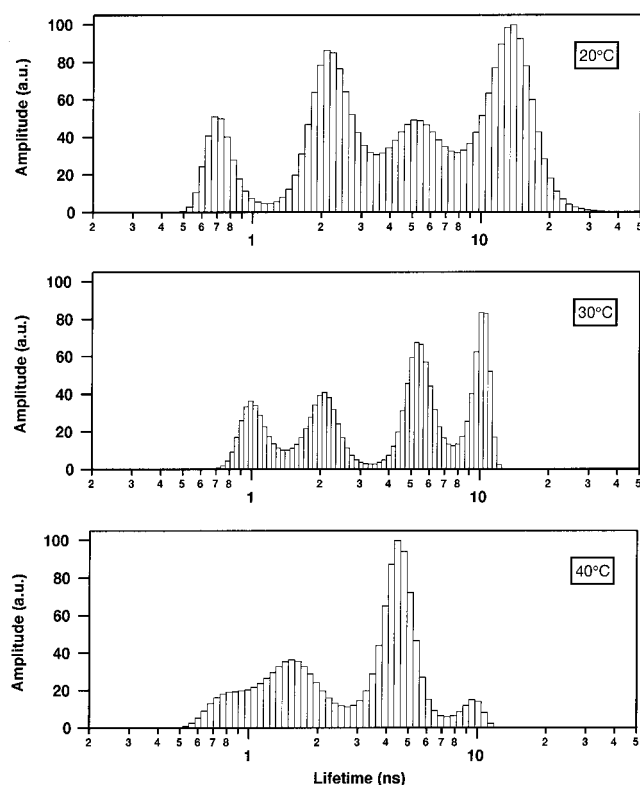


FIGURE 3 Effect of temperature on the lifetime distribution of *t*-PnA in POPC large unilamellar vesicles containing 15 mol% cholesterol at 600 bars.

when this amplitude reaches its maximum value,  $\chi_p^\beta = 1$ . Fig. 4 shows the variation of  $\chi^\beta$  at 1 atmosphere, 600 bars, and 800 bars, as a function of cholesterol concentration at 20°C. At 1 atm the membrane is entirely in the  $\beta$ -phase at a mole fraction cholesterol  $\chi_{\text{chol}} \approx 0.35$ . However, at 600 bars and 800 bars the cholesterol fractions necessary to form the  $\beta$ -phase are, respectively, 0.20 and 0.15. From these results, the pressure equivalent of cholesterol enrichment of POPC is 500 bars =  $0.13 \pm 0.02$  mole fraction cholesterol in the pressure range studied, which is lower than the value obtained for dilauroylphosphatidylcholine (500 bars = 0.19 mole fraction cholesterol; MacDonald et al., 1987) and dioleoylphosphatidylcholine (500 bars = 0.22 mole fraction cholesterol; Chong and Cossins, 1984) from steady-state fluorescence measurements. Similar plots were made at 30°C and 40°C, and, finally, the thermal phase diagram of the POPC/cholesterol mixture at several pressures was constructed. Fig. 5 shows this phase diagram at 1 atm and 600 bars. The figure shows that pressure shifts the phase diagram to lower cholesterol concentrations. In the same manner, a pressure/cholesterol concentration phase diagram was determined for each temperature (Fig. 6). From this phase diagram it is clear that pressure induces the formation of the  $\beta$ -phase and increases its fraction. However, the cholesterol fraction in both the  $\alpha$ - and  $\beta$ -phases decreases with increasing pressure. For example, in POPC liposomes containing 0.10 mole fraction cholesterol, the fraction of  $\beta$ -phase is

**TABLE 4** Fluorescence anisotropy decay parameters of *t*-PnA in LUVs of POPC as a function of cholesterol concentration and pressure, calculated according to the associative model

$\chi_{\text{chol}}$	$P$ (bar)	$\phi_{\alpha}$ (ns)	$\phi_{\beta}$ (ns)	$\phi_G$ (ns)	$r_{\infty}^{\alpha}$	$r_{\infty}^{\beta}$	$r_{\infty}^G$	$r(0)$	$\langle P_2 \rangle^{\alpha}$	$\langle P_2 \rangle^{\beta}$	$\langle P_2 \rangle^G$	$\chi^2$
0	1	1.5			0.07			0.28	0.42			1.02
	500	2.4			0.09			0.23	0.48			1.07
	900	1.6			0.13			0.23	0.58			1.06
0.1	1	0.8	2.0		0.10	0.12		0.32	0.51	0.55		1.02
	500	0.5	1.8		0.11	0.12		0.36	0.53	0.55		1.05
	900	0.4	1.2		0.12	0.18		0.4	0.56	0.68		1.26
0.2	1	0.2	1.2		0.13	0.16		0.4	0.58	0.64		1.12
	500	0.3	1.1		0.13	0.18		0.4	0.58	0.68		1.08
	900		2.3	0.1		0.16	0.23	0.4		0.64	0.77	1.08

$\langle P_2 \rangle^{\alpha}$ ,  $\langle P_2 \rangle^{\beta}$ , and  $\langle P_2 \rangle^G$  are, respectively, the order parameters of the probe in the  $\alpha$ -,  $\beta$ -, and gel phases.

$\phi$ ,  $\pm 0.5$

$\langle P_2 \rangle$ ,  $\pm 0.01$

$\chi^{\beta} = 0.04$ , and the fractions of cholesterol in the  $\alpha$ - and  $\beta$ -phases are, respectively,  $\chi_c^{\alpha} = 0.09 \pm 0.03$  and  $\chi_c^{\beta} = 0.33 \pm 0.02$  at atmospheric pressure. However,  $\chi^{\beta}$  increases to  $\sim 0.4$  when the lipid mixture is pressurized to 500 bars, and the  $\chi_c^{\alpha}$  and  $\chi_c^{\beta}$  values decrease to 0.03 and 0.21, respectively.

Additional information on the effect of pressure on the physical properties of this lipid mixture was obtained from the anisotropy experiments. These experiments support the existence of two phases with different order parameters that should be rather consistent with the  $\alpha$ - and  $\beta$ -phases.  $\langle P_2 \rangle^{\beta}$  is slightly higher than  $\langle P_2 \rangle^{\alpha}$  and lower than the value obtained for the same phase in dimyristoylphosphatidylcholine/cholesterol systems (Mateo et al., 1995). This result is logical, considering the structure of the unsaturated phospholipid, with a *cis* double bond, which should introduce important structural distortion into the lipid packing of the  $\beta$ -phase. In most cases pressure increases the orientational order of both  $\alpha$ - and  $\beta$ -phases. The effect of pressure on the  $\alpha$ -phase order parameter  $\langle P_2 \rangle^{\alpha}$  is lower than that observed in the pure fluid phase of POPC, because pressure, as was mentioned above, also changes the composition of these

phases, decreasing the cholesterol concentration. The rotational correlation times associated with the  $\beta$ -phase were higher than those corresponding to the  $\alpha$ -phase, suggesting a more fluid environment for the  $\alpha$ -phase. Because the errors in the determination of these rotational parameters are still rather large, it is not yet possible to draw any conclusions about their dependence on pressure.

In conclusion, the fluorescence lifetime distribution pattern of *t*-PnA in large unilamellar vesicles of POPC is clearly modulated by the temperature, pressure, and cholesterol concentration changes. From these lifetime distributions it is possible to quantify the effects of these three parameters on the lipid bilayer. An increase in pressure and a decrease in temperature have similar effects on the structure and composition of POPC/cholesterol mixtures. Both thermodynamic variables alter the structure, composition, and molar fraction of the  $\alpha$ - and  $\beta$ -phases. This work shows that very small changes in temperature, pressure, and/or cholesterol concentration induce perturbation of the local

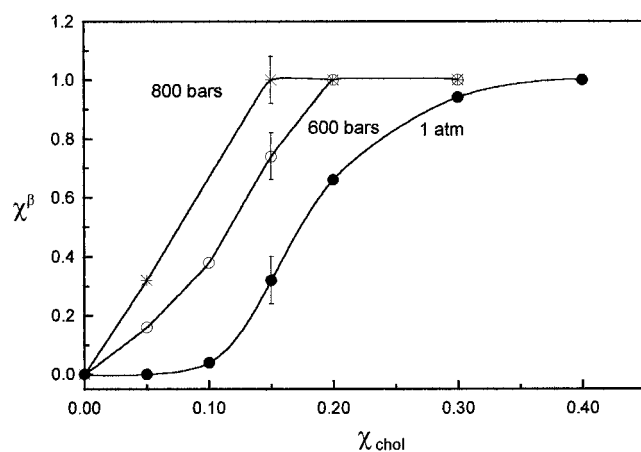


FIGURE 4 The  $\beta$ -phase fraction,  $\chi^{\beta}$ , of POPC/cholesterol mixtures at 1 atm, 600 bars, and 800 bars as a function of cholesterol concentration at 20°C.

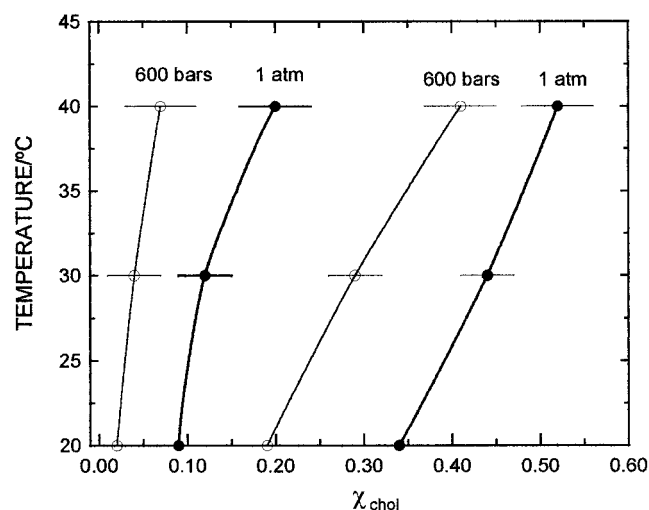


FIGURE 5 Effect of pressure on the thermotropic phase diagram of the POPC/cholesterol mixture. ●, Phase diagram constructed at atmospheric pressure from the lifetime distributions of *t*-PnA. ○, Data obtained at 600 bars (see text).

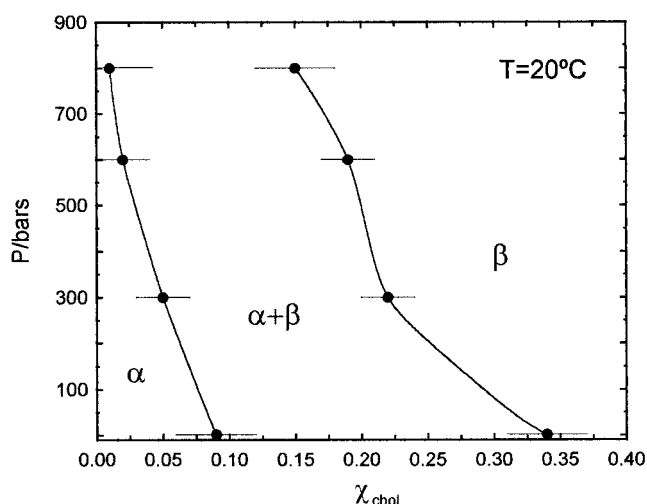


FIGURE 6 Pressure/cholesterol concentration phase diagram of POPC at 20°C.

fraction and composition of lateral domains, which can have important biochemical implications.

We thank P. Denjean for technical assistance in the laser operation at Ecole Normale Supérieure de Cachan.

This work was supported by the France-Spain scientific cooperation program "PICASSO."

## REFERENCES

- Almeida, P. F. F., W. L. C. Vaz, and T. E. Thompson. 1992. Lateral diffusion in the liquid phases of dimyristoylphosphatidylcholine/cholesterol lipid bilayers: a free volume analysis. *Biochemistry*. 31: 6739–6747.
- Alvia, R. C., C. C. Cortain, and L. M. Gordon, editors. 1988. *Lipid Domains and the Relationship to Membrane Function*. Liss, New York.
- Brochon, J. C. 1994. Maximum entropy method of data analysis in time-resolved anisotropy. *Methods Enzymol.* 240:262–311.
- Chong, P.-L. G., and A. R. Cossins. 1984. Interacting effects of temperature, pressure and cholesterol content upon the molecular order of dioleoylphosphatidylcholine vesicles. *Biochim. Biophys. Acta*. 772: 197–201.
- Gordon, L. M., P. W. Mobley, J. A. Esgate, G. Hoffman, A. D. Whetton, and M. D. Housley. 1983. Thermotropic lipid phase separation in human platelet and rat liver plasma membrane. *J. Membr. Biol.* 76:139–149.
- Gull, S. F. 1989. Developments in maximum entropy data analysis. In *Maximum Entropy, and Bayesian Methods*. J. Skilling, editor. Kluwer Academic Publishers, Dordrecht, The Netherlands. 53–71.
- Hope, M. J., M. B. Bally, G. Webb, and P. R. Cullis. 1985. Production of large unilamellar vesicles by a rapid extrusion procedure. Characterisation of size distribution, trapped volume and ability to maintain a membrane potential. *Biochim. Biophys. Acta*. 812:55–65.
- Hudson, B. S., and S. A. Cavalier. 1988. Studies of membrane dynamics and lipid-protein interactions with parinaric acid. In *Spectroscopic Membrane Probes*, Vol. 1. L. M. Loew, editor. CRC Press, Boca Raton, FL. 43–62.
- Livesey, A. K., and J. C. Brochon. 1987. Analyzing the distribution of decay constants in pulse-fluorimetry using the maximum entropy method. *Biophys. J.* 52:693–706.
- MacDonald, A. G., K. W. J. Wahle, A. R. Cossins, and M. K. Behan. 1987. Temperature, pressure and cholesterol effects on bilayer fluidity: a comparison of pyrene excimer/monomer ratios with the steady state fluorescence polarization of diphenylhexatriene in liposomes and microsome. *Biochim. Biophys. Acta*. 938:231–242.
- Mateo, C. R., A. U. Acuña, and J. C. Brochon. 1995. Liquid-crystalline phases of cholesterol/lipid bilayers as revealed by the fluorescence of *trans*-parinaric acid. *Biophys. J.* 68:978–987.
- Mateo, C. R., J. C. Brochon, M. P. Lillo, and A. U. Acuña. 1993a. Lipid bilayer lateral clustering as detected by the fluorescence kinetics and anisotropy of *trans*-parinaric acid. *Biophys. J.* 65:2237–2247.
- Mateo, C. R., M. P. Lillo, J. González-Rodríguez, and A. U. Acuña. 1991. Lateral heterogeneity in human platelet plasma membranes and lipid from the time-resolved fluorescence of *trans*-parinaric acid. *Eur. Biophys. J.* 20:53–59.
- Mateo, C. R., P. Tauc, and J. C. Brochon. 1993b. Pressure effects on the physical properties of lipid bilayers detected by *trans*-parinaric acid fluorescence decay. *Biophys. J.* 65:2248–2260.
- Naqvi, K. R. 1981. Photoselection in uniaxial liquid crystals: the advantages of using saturation light pulses for the determination of orientational order. *J. Chem. Phys.* 74:2658–2659.
- Recktenwald, D. J., and H. M. McConnell. 1981. Phase equilibria in binary mixtures of phosphatidylcholine and cholesterol. *Biochemistry*. 20: 4505–4510.
- Sankaram, M. B., and T. E. Thompson. 1990. Interactions of cholesterol with various glycerophospholipids and sphingomyelin. *Biochemistry*. 29:10670–10675.
- Schroeder, F., J. R. Jefferson, A. B. Kier, J. Knittel, T. J. Scallen, W. Gibson, M. Wood, and I. Hapala. 1991. Membrane cholesterol dynamics: cholesterol domains and kinetics pools. *Proc. Soc. Exp. Biol. Med.* 196:235–252.
- Shang, Q.-Y., X. Dou, and B. S. Hudson. 1991. Off axis orientation of the electronic transition moment for a linear conjugated polyene. *Nature*. 352:703–705.
- Singer, S. J., and G. L. Nicolson. 1972. The fluid mosaic model of the structure of cell membranes. *Science*. 175:720–731.
- Skilling, J. 1989. Classic maximum entropy. In *Maximum Entropy, and Bayesian Methods*. J. Skilling, editor. Kluwer Academic Publishers, Dordrecht, The Netherlands. 45–52.
- Skilling, J. 1991. Fundamentals of MaxEnt in data analysis. In *Maximum Entropy in Action*. B. Buck and V. A. Macaulay, editors. Clarendon, Oxford University Press, Oxford. 19–40.
- Vist, M. R., and J. H. Davis. 1990. Phase equilibria of cholesterol/dipalmitoylphosphatidylcholine mixtures:  $^2\text{H}$  nuclear magnetic resonance and differential scanning calorimetry. *Biochemistry*. 29:451–464.
- Welti, R., and D. F. Silbert. 1982. Partition of parinoyl phospholipid probes between solid and fluid phosphatidylcholine phases. *Biochemistry*. 21: 5685–5689.
- Wolf, D. E., and J. K. Voglmayr. 1984. Diffusion and regionalization in membranes of maturing rat spermatozoa. *J. Cell. Biol.* 98:1678–1684.
- Yechiel, E., and M. Edidin. 1987. Micrometer scale domains in fibroblast plasma membranes. *J. Cell Biol.* 105:755–760.